

Active Biopolymers Confer Fast Reorganization Kinetics

Douglas Swanson*

Department of Physics, Princeton University, Princeton, New Jersey, USA

Ned S. Wingreen†

Department of Molecular Biology, Princeton University, Princeton, New Jersey, USA

Many cytoskeletal biopolymers are “active,” consuming energy in large quantities. In this Letter, we identify a fundamental difference between active polymers and passive, equilibrium polymers: for equal mean lengths, active polymers can reorganize faster than equilibrium polymers. We show that equilibrium polymers are intrinsically limited to linear scaling between mean lifetime and mean length, MFPT $\sim \langle L \rangle$, by analogy to 1-d Potts models. By contrast, we present a simple active-polymer model that improves upon this scaling, such that MFPT $\sim \langle L \rangle^{1/2}$. Since to be biologically useful, structural biopolymers must typically be many monomers long, yet respond dynamically to the needs of the cell, the difference in reorganization kinetics may help to justify active polymers’ greater energy cost. PACS numbers: 87.10.Ed, 87.16.ad, 87.16.Ln

Cytoskeletal polymers play a key role in cellular reproduction, locomotion, and transport [1–3]. Biopolymers like actin filaments and microtubules in eukaryotes and FtsZ, MreB, and ParM in prokaryotes grow by accumulating monomers bound to the nucleotide triphosphates ATP or GTP. The monomers hydrolyze these triphosphates to the diphosphates ADP or GDP, consuming energy in an irreversible process and inducing conformational changes that destabilize the polymers. In some cells, cytoskeletal ATP consumption can approach 50% of total cellular ATP consumption [4, 5]. What advantage do active polymers offer over passive, equilibrium polymers to justify this costly energy expenditure?

We highlight a fundamental difference between active and equilibrium polymers: active polymers can reorganize faster than equilibrium polymers. Moreover, this difference in reorganization times widens as mean polymer length grows. Since biological structures like mitotic spindles or pseudopods must reach a certain size to accomplish their function, yet be quickly deconstructed and reorganized, this intrinsic difference may at least partly justify active polymers’ greater energy cost.

A large class of equilibrium models describes a polymer as an ordered sequence of monomers, each of one of q types (including different conformational states of the same molecule). Monomers can attach, detach, and potentially interconvert among the q types. Interactions between neighboring monomers $\{i, i+1\}$ contribute free energy $J_{\{i, i+1\}}$ to the total free energy of the polymer. Such models can also describe polymers consisting of bundles of k protofilaments, by increasing the number of “monomer” types to q^k . These models are generalizations of 1-d, q^k -state Potts models [6]. The free energy of an equilibrium polymer in these models scales as the polymer length L for large L , specifically $\mathcal{F} \approx L\lambda_{\max}$, where λ_{\max} is the largest eigenvalue of the transfer matrix [7]. Hence, the equilibrium distribution of polymer lengths will be exponential, $p(L) \sim e^{-L/\langle L \rangle}$, with a character-

istic mean length $\langle L \rangle = \frac{kT}{\lambda_{\max}}$. Because for large L the free energy effectively depends on only the largest eigenvalue λ_{\max} , the dynamics are essentially one-dimensional even for polymer bundles. This means that the effective force $-\frac{d\mathcal{F}}{dL} \approx -\lambda_{\max}$ is constant, generating a constant negative-velocity drift in the polymer length, with drift velocity $v_d \propto -\lambda_{\max}$. (Polymers maintain a finite equilibrium distribution because this negative drift is balanced by diffusion and nucleation of new polymers.) Importantly, since the polymer length drifts towards zero at constant negative drift velocity, starting from the nucleation length L_{nucl} , the mean polymer lifetime scales as $\frac{L_{\text{nucl}}}{|v_d|} \propto \frac{1}{\lambda_{\max}} \propto \langle L \rangle$. Thus the mean polymer lifetime or “mean first-passage time” (MFPT) scales as the mean length $\langle L \rangle$ for equilibrium polymers. This linear scaling is a fundamental limit for an equilibrium polymer. In order to improve upon it, a biological system must employ active or out-of-equilibrium processes. As an example, we present a simple active-polymer model based on microtubule dynamics that yields MFPT $\sim \langle L \rangle^{1/2}$.

Microtubule growth and disassembly dynamics have been well-studied [8–10]. In microtubules (and ParM), GTP hydrolysis leads to stochastic rapid disassembly of the entire polymer in a process called dynamic instability; the classic experimental results [11] are reviewed in [1]. Recent detailed models aim to explain specific aspects of the experimental data [12–16]. We consider instead a minimal microtubule model [17] that incorporates dynamic instability. Specifically, we model an active polymer as an ordered sequence of monomers, each of which is bound either to GTP or GDP (Fig. 1). We call the group of GTP-bound monomers at the front of the polymer the “cap” and denote its size by x . We denote the total number of monomers (the polymer length) by L . GTP-bound monomers bind and unbind at the front end of the polymer with rates k_+ and k_- , respectively (Fig. 1A). GTP-bound monomers at the back of the polymer cap undergo hydrolysis to become GDP-bound

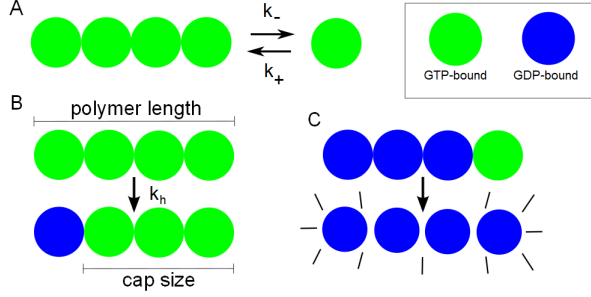


Figure 1: Schematic of growth and disassembly of a model active polymer. (A) GTP-bound monomers (green) bind and unbind at the front end of the polymer. (B) The last GTP-bound monomer at the back of the “cap” undergoes hydrolysis to become an GDP-bound monomer (blue), decreasing the cap size by one. (C) If the cap size shrinks to zero, the polymer completely disassembles.

monomers with rate k_h (Fig. 1B). If the cap size shrinks to zero, the polymer completely disassembles (Fig. 1C). New polymers of length and cap size 2 are nucleated with rate k_{nucl} . We call the concentration of free GTP-bound monomers c and analytically treat the mean-field regime where c is constant, a good approximation for eukaryotic cells where the number of monomers is typically large ($\sim 10^6$). For comparison, we also consider an equilibrium polymer that obeys the same rules but without hydrolysis so that its length and cap size are equal. We show explicitly that this particular equilibrium model satisfies the general equilibrium scaling relation $\text{MFPT} \sim \langle L \rangle$.

The exact master equation for the concentration $C_{L,x}$ of polymers of length L and cap size x is

$$\frac{d}{dt}C_{L,x} = k_+c(C_{L-1,x-1} - C_{L,x}) + k_-(C_{L+1,x+1} - C_{L,x}) + k_h(C_{L,x+1} - C_{L,x}) + k_{\text{nucl}}c^2\delta_{L,2}\delta_{x,2}. \quad (1)$$

Coarse-graining this equation leads to a continuum Fokker-Planck (FP) description of the probability $p = p(x, L, t)$ that a single active polymer will have length L and cap size x at a time t after its birth:

$$\frac{\partial p}{\partial t} = D \frac{\partial^2 p}{\partial x^2} + D_{LL} \frac{\partial^2 p}{\partial L^2} + D_{xL} \frac{\partial^2 p}{\partial x \partial L} - a \frac{\partial p}{\partial x} - g \frac{\partial p}{\partial L}, \quad (2)$$

where $D = D_{xx} = \frac{1}{2}(k_+c + k_- + k_h)$, $D_{LL} = \frac{1}{2}(k_+c + k_-)$, and $D_{xL} = k_+c + k_-$ are diffusion coefficients, $a = k_+c - k_- - k_h$ is the cap drift velocity ($a < 0$), and $g = k_+c - k_-$ is the length drift velocity. The FP equation (2) describes the time-evolution of an individual polymer born at time 0 (the time coordinate t represents polymer age). In the mean-field regime each polymer evolves independently once nucleated, and hence the k_{nucl} term does not appear (for details see [18]). Assuming $g \gg -a$, the effect of cap diffusion dominates the effect of length diffusion, and so we may neglect the D_{LL}

and D_{xL} terms [18]. Solving the FP equation (2) yields

$$p(x, L, t) = \frac{1}{\sqrt{4\pi Dt}} e^{-\frac{(x-at-2)^2}{4Dt}} \left(1 - e^{-\frac{2x}{Dt}}\right) \delta(L - gt - 2), \quad (3)$$

where the initial condition is $p(x, L, 0) = \delta(x-2)\delta(L-2)$, *i.e.* polymers nucleate with length and cap size 2, and the boundary condition is $p(0, L, t) = 0$, *i.e.* polymers with cap size zero disassemble. (Changing the nucleation size does not affect any essential results.)

The distribution of polymer lifetimes or “first-passage times” (FPTs) is

$$P_{\text{FPT}}(t) = -\frac{d}{dt} \iint_0^\infty p(x, L, t) dx dL = \frac{1}{\sqrt{\pi Dt^3}} e^{-\frac{(at+2)^2}{4Dt}}, \quad (4)$$

and the mean first-passage time (MFPT) has the simple form $\text{MFPT} = -2/a$. The steady-state polymer length distribution is

$$P_{\text{active}}(L) = \iint_0^\infty p(x, L, t) dx dt, \quad (5)$$

yielding the active-polymer average length

$$\langle L \rangle_{\text{active}} = \int_0^\infty P_{\text{active}}(L) L dL = \frac{g(D-a)}{a^2}, \quad (6)$$

so that for long polymers ($\langle L \rangle \gg 1, |a| \ll 1$), one finds $\langle L \rangle \simeq gD/a^2$, and therefore $\text{MFPT} = -2/a \sim \langle L \rangle^{1/2}$ to leading order. This sublinear scaling requires some non-equilibrium process, here the irreversible hydrolysis of monomers. Note that the details of the non-equilibrium model do matter to the degree of sublinearity; for example, a more realistic microtubule model [17] yields $\text{MFPT} \sim \langle L \rangle^{0.7}$ [18].

By comparison, in the equilibrium limit of this model the cap is the entire polymer. Dropping the d/dL terms in (2) yields an equilibrium solution that looks like (3) without the factor $\delta(L - gt - 2)$. The equilibrium length distribution can then be obtained by integrating over polymer age:

$$P_{\text{equil}}(L) = -\frac{a}{D} e^{aL/D}, \quad (7)$$

and the equilibrium-polymer average length is $\langle L \rangle_{\text{equil}} = -D/a$. Hence, we recover the linear scaling $\text{MFPT} \sim \langle L \rangle$ expected for equilibrium polymers.

To validate these scaling relations, the master equation (1) was simulated using the Gillespie algorithm [19]. The monomer addition rate k_+ was held fixed throughout the simulations. For equilibrium polymers we set $k_h = 0$, while for active polymers for simplicity we set $k_- = 0$. The nucleation rate k_{nucl} was tuned to hold the steady-state fraction of polymerized material constant at 75%, with k_{nucl} from 10^{-5} to 10^{-8} . This is in line with experimentally measured values for microtubules [20]. (Changing the fraction of polymerized material to 95% does not

affect the qualitative results [18].) This leaves a single free parameter, k_- for equilibrium polymers and k_h for active polymers, to control the polymer length and MFPT. With only a single free parameter, each system is fully constrained by holding either the MFPT or the average length fixed, thus yielding a fair comparison between the equilibrium and active polymers.

Figure 2A shows the MFPT of the equilibrium and active polymers as functions of their average length. The data points are from simulations using 400,000 monomers; the curves are from $\text{MFPT} = -2/a$ combined with $\langle L \rangle_{\text{equil}} = -D/a$ and (6) for $\langle L \rangle_{\text{active}}$. The MFPT scales $\sim \langle L \rangle$ for equilibrium polymers and $\sim \langle L \rangle^{1/2}$ for active polymers as expected. Hence, for the same average length, the active polymers have much shorter mean lifetimes than the equilibrium polymers, and this difference widens as average length grows. Figure 2B compares length distributions for the equilibrium and active polymers with the same MFPT ($\simeq 10$). Theoretical results from (5) and (7) are shown in black. Agreement between simulation and theory is excellent, validating our use of the FP equation. (For a comparison of length distributions with the same $\langle L \rangle$, see [18].)

What might be the biological consequences of the different equilibrium and active polymer scaling relations? To address this question, we examine the time scale for large-scale spatial reorganization of structures, *i.e.* the time needed for a system to disassemble polymers at one site, move the material to another site, and reassemble new polymers. Cells often accomplish large-scale polymer reorganization *in vivo* by spatially regulating nucleation [21–23]. To model such regulation simply, we consider two spatial sites. We start simulations with nucleation occurring only at site 1, allow the system to come to steady state, then switch off nucleation at site 1 and switch on nucleation at site 2. Monomers are assumed to transition between the two sites with a “diffusion” rate k_D , while polymers do not diffuse. We define the “reorganization time” as the time needed after the nucleation switch for 50% of the final steady-state amount of polymerized material to assemble at site 2. Initially we assume diffusion to be fast ($k_D = \infty$) so that a single effective pool of free monomers is shared between the two sites, and then we consider the more biologically-relevant finite-diffusion regime.

Figure 2C shows the reorganization time for our simple equilibrium and active polymers as functions of their average length, with fast diffusion. The reorganization time scales $\sim \langle L \rangle^2$ for the equilibrium polymers and $\sim \langle L \rangle$ for the active polymers. Hence, for a given average length, the active polymers reorganize faster than the equilibrium polymers, and like for the MFPT the difference widens with increasing average length. The scaling exponents differ from those for the MFPT because the reorganization time is dominated by a few very long-lived

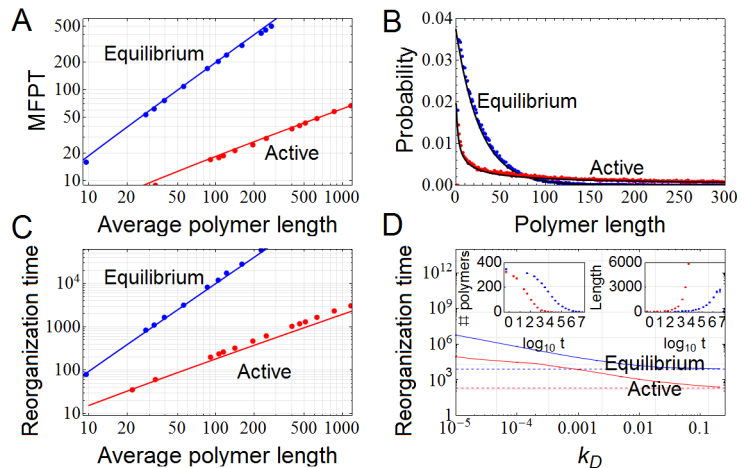


Figure 2: Lifetimes versus length for equilibrium (blue) and active (red) polymers. (A) Mean first-passage time (MFPT) to polymer disassembly versus average length. The monomer addition rate k_+ is held fixed, and time is always measured in units of $(k_+c)^{-1}$, the mean time for monomer binding. Solid lines are fits to theory with slopes 1 and 0.5 for equilibrium and active polymers, respectively. Some error bars are smaller than data-point symbols. (B) Length distributions with $\text{MFPT} \simeq 10$, with theoretical fits (black) from (5) and (7). The equilibrium polymers have average length 30, while the active polymers have average length 600. (C) Reorganization time (defined in text) versus average length. Solid lines are theoretical fits from (8) with slopes 2 and 1 for equilibrium and active polymers, respectively. (D) Reorganization time versus monomer diffusion constant. Dashed lines show infinite-diffusion limits. Insets: time series showing average polymer number (left) and average polymer length (right) at site 1 versus time after nucleation is switched off.

long polymers, whereas the MFPT is dominated by many short-lived short polymers.

To understand the scaling relations in Fig. 2C, we estimate the reorganization time analytically as half the “average material age,” which we define as the average age of the polymers in a steady-state snapshot of the system, weighted by the length of each polymer:

$$\tau_{\text{reorg}} \approx \frac{1}{2} \frac{\int_0^\infty \text{age}(L) P(L) L dL}{\int_0^\infty P(L) L dL}. \quad (8)$$

This average material age captures the amount of time an average monomer spends in an active polymer before it turns over, and well-approximates the reorganization time. Long polymers have more material than short polymers, and so the average material age is weighted by the length of each polymer. For our equilibrium polymers, $\text{age}(L) = -L/a$, which gives $\tau_{\text{reorg}}^{\text{equil}} \approx 2D/a^2 \sim \langle L \rangle^2$. Indeed, since the drift velocity $a \sim 1/\langle L \rangle$ for any equilibrium polymer model as discussed above, $\text{age}(L) \sim L^2$, and thus the equilibrium reorganization time scales generally $\sim \langle L \rangle^2$. As for the MFPT, this scaling is a fundamental property of equilibrium polymers. To im-

prove upon it requires active energy-dissipation or some non-equilibrium process. For example, our simple active polymers have $\text{age}(L) = L/g$ and hence $\tau_{\text{reorg}}^{\text{active}} \approx \frac{4(a^2 - 3aD + 3D^2)}{3a^2(D-a)}$, so that for large $\langle L \rangle$ with $|a| \ll 1$, $\tau_{\text{reorg}}^{\text{active}} \approx 4D/a^2 \sim \langle L \rangle$.

Next we consider the effects of slow monomer diffusion. Figure 2D shows the reorganization time versus the monomer transition rate k_D between sites for equilibrium and active polymers with the same average length ($\simeq 90$) and fraction of polymerized material (75%). The fast-diffusion limits, which are reached for $k_D \simeq 1$ (in units of k_+c), are shown with dashed lines. Strikingly, the active polymers still reorganize much faster than the equilibrium polymers even when slow diffusion limits the reorganization time. To understand this effect, consider the equilibrium polymer dynamics after nucleation is switched off at site 1: polymers there disassemble stochastically and, since diffusion is slow, the released monomers typically rejoin other polymers at the same site. Hence the number of polymers at site 1 drops rapidly while the average polymer length grows (Fig. 2D, insets). Eventually site 1 has only a few very long polymers. The equilibrium polymers remain in this state for a very long time, exchanging monomers with the free monomer pool at site 1 while diffusion slowly drains the pool, until the polymers finally disassemble. Therefore, the time needed for slow diffusion to move half the monomers from site 1 to site 2 is a good rough approximation for the equilibrium reorganization time [18]. In contrast, active polymers do not release monomers to the free monomer pool except by disassembly. After the switch in nucleation, the number of active polymers at site 1 drops while the average length grows, similar to the equilibrium polymers. However, the few long-lived active polymers at site 1 then quickly accumulate and hydrolyze all the free monomers there, and then all the polymers disassemble. The time to hydrolyze all the monomers at site 1, plus the time for half of those monomers to diffuse to site 2, is therefore a good rough approximation for the active reorganization time [18].

In summary, we find a fundamental difference between active and equilibrium polymers: active polymers can reach a fixed mean length with faster reorganization kinetics than equilibrium polymers. Very generally, we show that equilibrium polymer lifetimes scale linearly with mean length. In contrast, active polymer lifetimes can scale sublinearly, for example as $\langle L \rangle^{1/2}$ in a simple model motivated by microtubules or as $\langle L \rangle^{0.7}$ in a more realistic model [17, 18]. Furthermore, in our example the kinetic advantage of active polymers persists even for slow monomer diffusion. In a dynamic cellular environment, this kinetic advantage may help justify active polymers' greater energy cost.

Our comparison of active and equilibrium polymers predicts one might find equilibrium polymers in biologi-

cal contexts where polymer turnover is slow or structures rarely need to be reorganized. This may be the case for eukaryotic intermediate filaments [24] or for the bacterial homolog crescentin [25]. In addition, the existence of proteins like formins and profilins that accelerate actin polymerization suggests that kinetic regulation of active polymers is important to cells. Finally, although the specific active model we consider is most closely based on polymers like microtubules or ParM that exhibit dynamic instability, our conclusions regarding accelerated kinetics could also relate to actin networks for which branching plays a role analogous to nucleation [26].

Our model neglects many complexities of real biopolymers; clearly active polymers accomplish more than simply reaching a certain length with a certain lifetime. We only suggest that fast reorganization kinetics might be a general (and generally desirable) feature of the active polymer systems that are ubiquitous in biology.

We thank William Bialek, Zemer Gitai, Joshua Shaevitz, and Sven van Teeffelen for helpful suggestions. D.S. was supported by a National Science Foundation Graduate Research Fellowship and N.S.W. by National Science Foundation Grant No. PHY-0957573.

* Electronic address: dsswanso@princeton.edu

† Electronic address: wingreen@princeton.edu

- [1] A. Desai and T. J. Mitchison, *Annu. Rev. Cell Dev. Biol.* **13**, 1 (1997).
- [2] T. D. Pollard and J. A. Cooper, *Science* **326**, 5957 (2009).
- [3] M. T. Cabeen and C. Jacobs-Wagner, *Annu. Rev. Genet.* **44**, 1 (2010).
- [4] J. L. Daniel, I. R. Molish, L. Robkin, and H. Holmsen, *Eur. J. Biochem.* **156**, 3 (1986).
- [5] B. W. Bernstein and J. R. Bamberg, *J. Neurosci.* **23**, 1 (2003).
- [6] F. Y. Wu, *Rev. Mod. Phys.* **54**, 1 (1982).
- [7] P. M. Chaikin and T. C. Lubensky, *Principles of Condensed Matter Physics* (2000).
- [8] T. Mitchison and M. Kirschner, *Nature* **312**, 5591 (1984).
- [9] P. Bayley, M. Schilstra, and S. Martin, *FEBS Lett.* **259**, 1 (1989).
- [10] F. Verde, M. Dogterom, E. Stelzer, E. Karsenti, and S. Leibler, *J. Cell Biol.* **118**, 5 (1992).
- [11] R. A. Walker, E. T. O'Brien, N. K. Pryer, M. F. Soboeiro, W. A. Voter, H. P. Erickson, and E. D. Salmon, *J. Cell Biol.* **107**, 4 (1988).
- [12] I. M. Jánosi, D. Chrétien, and H. Flyvbjerg, *Biophys. J.* **83**, 3 (2002).
- [13] T. Antal, P. K. Krapivsky, S. Redner, M. Mailman, and B. Chakraborty, *Phys. Rev. E* **74**, 14 (2007).
- [14] P. Hinow, V. Rezania, and J. A. Tuszyński, *Phys. Rev. E* **80**, 031904 (2009).
- [15] L. Brun, B. Rupp, J. J. Ward, and F. Nédélec, *Proc. Natl. Acad. Sci. U.S.A.* **106**, 50 (2009).
- [16] P. Ranjith, D. Lacoste, K. Mallick, and J-F. Joanny, *Biophys. J.* **96**, 2146 (2009).
- [17] H. Flyvbjerg, T. E. Holy, and S. Leibler, *Phys. Rev. Lett.*

- 73**, 17 (1994).
- [18] See supplementary material at [link].
- [19] D. T. Gillespie, *J. Phys. Chem.* **81**, 25 (1977).
- [20] W. Beertsen, J. N. M. Heersche, and J. E. Aubin, *J. Cell Biol.* **95**, 2 (1982).
- [21] C. E. Oakley and B. R. Oakley, *Nature* **338**, 6217 (1989).
- [22] L. M. Machesky, R. D. Mullins, H. N. Higgs, D. A. Kaiser, L. Blanchoin, R. C. May, M. E. Hall, and T. D. Pollard, *Proc. Natl. Acad. Sci. U.S.A.* **96**, 7 (1999).
- [23] V. Malikov, A. Kashina, and V. Rodionov, *Mol. Biol. Cell* **15**, 6 (2004).
- [24] K. H. Yoon, M. Yoon, R. D. Moir, S. Khuon, F. W. Flitney, and R. D. Goldman, *J. Cell Biol.* **153**, 3 (2001).
- [25] G. Charbon, M. T. Cabeen, and C. Jacobs-Wagner, *Genes Dev.* **23**, 9 (2009).
- [26] T. D. Pollard, *Annu. Rev. Biophys. Biomol. Struct.* **36**, 1 (2007).

Supplementary Information for: Active Biopolymers Confer Fast Reorganization Kinetics

Douglas Swanson*

Department of Physics, Princeton University, Princeton, New Jersey, USA

Ned S. Wingreen†

Department of Molecular Biology, Princeton University, Princeton, New Jersey, USA

Here we solve the full Fokker-Planck equation defined in the main text, and justify the simplifications employed there. Next, we estimate the reorganization time for polymers to disassemble at one spatial site and reassemble at another spatial site, for slow monomer diffusion. We then compare equilibrium and active-polymer length distributions with the same average length, and also consider the result of varying the steady-state fraction of polymerized material. Finally, we obtain scaling relations for a more realistic model of microtubule dynamics [1], and demonstrate that an equilibrium two-species model satisfies our predicted equilibrium scaling relation.

FOKKER-PLANCK DERIVATION

Here we solve the full Fokker-Planck equation (2) defined in the main text, and justify the simplifications leading to (3). The Fokker-Planck equation for the probability $p = p(x, L, t)$ of finding a polymer with length L and cap size x at a time t after the polymer's birth is

$$\frac{\partial p}{\partial t} = D_{xx} \frac{\partial^2 p}{\partial x^2} + D_{LL} \frac{\partial^2 p}{\partial L^2} + D_{xL} \frac{\partial^2 p}{\partial x \partial L} - a \frac{\partial p}{\partial x} - g \frac{\partial p}{\partial L}, \quad (\text{S1})$$

where $D_{xx} = \frac{1}{2}(k_+c + k_- + k_h)$, $D_{LL} = \frac{1}{2}(k_+c + k_-)$, and $D_{xL} = k_+c + k_-$ are diffusion coefficients, $a = k_+c - k_- - k_h$ is the cap drift velocity ($a < 0$), and $g = k_+c - k_-$ is the length drift velocity. This equation does not contain a term proportional to k_{nuc} . The master equation (1) describes the time-evolution of an entire system of polymers (the time coordinate t represents wall-clock time), whereas the Fokker-Planck equation (2) describes the time-evolution of an individual polymer born at time 0 (the time coordinate t represents polymer age). In the mean-field regime we treat, the growth of an individual polymer born at time 0 is completely independent of the other polymers in the system (i.e. once nucleated, each polymer evolves independently). Therefore, the nucleation rate k_{nuc} does not explicitly affect the normalized distributions of polymer lengths, caps, or lifetimes. However, the nucleation rate does affect the steady-state amount of polymerized material and hence the free monomer concentration c , in cases where c is allowed to vary.

The general solution to the Fokker-Planck equation (2) is

$$p(x, L, t) = \frac{1}{2\pi t \sqrt{4D_{xx}D_{LL} - D_{xL}^2}} \exp \left[-\frac{D_{xx}(L-gt-2)^2 + D_{LL}(x-at-2)^2 - D_{xL}(L-gt-2)(x-at-2)}{(4D_{xx}D_{LL} - D_{xL}^2)t} \right] \left(1 - e^{-\frac{2x}{D_{xx}t}} \right), \quad (\text{S2})$$

which satisfies both the initial condition $p(x, L, 0) = \delta(x-2)\delta(L-2)$ and the boundary condition $p(0, L, t) = 0$. In the limit $D_{LL} = D_{xL} = 0$, this reduces exactly to (3). We note that we have solved (S1) subject to no boundary conditions on L . This is a valid assumption for our active polymers, which nucleate with length $L_{\text{nuc}} = 2$ and then grow at average rate $g > 0$, and therefore the effect of the physical boundary condition at $L = 0$ is negligible. More formally, this assumption is valid provided $g \gg -a$, which implies the hydrolysis rate $k_h \gg -a$. The probability that a polymer is still alive, *i.e.* has not disassembled, by age t is

$$P_{\text{alive}}(t) = \int_0^\infty \int_0^\infty p(x, L, t) dx dL, \quad (\text{S3})$$

and the distribution of polymer lifetimes or “first-passage times” is

$$P_{\text{FPT}}(t) = -\frac{d}{dt} P_{\text{alive}}(t) = \frac{1}{\sqrt{\pi D_{xx} t^3}} e^{-\frac{(at+2)^2}{4D_{xx}t}}, \quad (\text{S4})$$

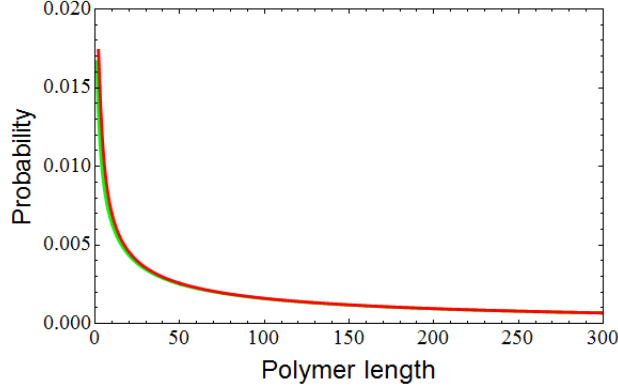


Figure S1: Comparison of active-polymer length distributions for $\langle L \rangle \simeq 132$. Length distributions were calculated from Fokker-Planck theory using the full joint distribution of polymer length and polymer age (S6) in red and the delta-function approximation $p(L, t) = P_{\text{alive}}(t) \cdot \delta(L - gt - 2)$ used in the main text (5) in green.

which is identical to (4) in the main text. Finally, in order to calculate the steady-state polymer length distribution (5), we require the joint distribution $p(L, t)$ between active polymer length L and age t . This may be obtained by integrating (S2) over cap sizes:

$$p(L, t) = \int_0^\infty p(x, L, t) dx, \quad (\text{S5})$$

and then the length distribution is

$$P_{\text{active}}(L) = \int_0^\infty p(L, t) dt. \quad (\text{S6})$$

In the limit $D_{LL} = D_{xL} = 0$ employed in the main text, the joint distribution $p(L, t) = P_{\text{alive}}(t) \cdot \delta(L - gt - 2)$. Figure S1 shows a direct comparison of the length distributions using both the full joint distribution (S6) in red and the delta-function approximation $p(L, t) = P_{\text{alive}}(t) \cdot \delta(L - gt - 2)$ used in the main text (5) in green. The length distributions are nearly identical, providing a practical validation for the intuitive simplifications used to obtain (3)-(6) in the main text. Inserting the delta-function approximation into (S6) gives

$$P_{\text{active}}(L) = \frac{1}{g} P_{\text{alive}}\left(\frac{L}{g}\right) \quad (\text{S7})$$

and the mean polymer length is calculated by integration by parts:

$$\langle L \rangle = \frac{\int_0^\infty L P_{\text{active}}(L) dL}{\int_0^\infty P_{\text{active}}(L) dL} = \frac{\int_0^\infty L P_{\text{alive}}\left(\frac{L}{g}\right) dL}{\int_0^\infty P_{\text{alive}}\left(\frac{L}{g}\right) dL} = \frac{1}{2} \frac{\int_0^\infty L^2 P_{\text{FPT}}\left(\frac{L}{g}\right) dL}{\int_0^\infty L P_{\text{FPT}}\left(\frac{L}{g}\right) dL} = \frac{g(D - a)}{a^2}. \quad (\text{S8})$$

More formally, we may argue that the effect of cap diffusion dominates the effect of length diffusion. Motivated by the scaling relations found in the main text (and the fact that the average cap size $\langle x \rangle = -\frac{D}{a} \sim \langle L \rangle^{1/2}$), we make the ansatz that we may rescale L to $\tilde{L} = L/\langle L \rangle$ and x to $\tilde{x} = x/\langle L \rangle^{1/2}$. Then we obtain the non-dimensionalized Fokker-Planck equation:

$$\frac{\partial p}{\partial t} = \frac{D_{xx}}{\langle L \rangle} \frac{\partial^2 p}{\partial \tilde{x}^2} + \frac{D_{LL}}{\langle L \rangle^2} \frac{\partial^2 p}{\partial \tilde{L}^2} + \frac{D_{xL}}{\langle L \rangle^{3/2}} \frac{\partial^2 p}{\partial \tilde{x} \partial \tilde{L}} - \frac{a}{\langle L \rangle^{1/2}} \frac{\partial p}{\partial \tilde{x}} - \frac{g}{\langle L \rangle} \frac{\partial p}{\partial \tilde{L}}. \quad (\text{S9})$$

For long polymers ($\langle L \rangle \gg 1$) the D_{LL} and D_{xL} terms will be much smaller than the remaining three terms, and we may neglect the D_{LL} and D_{xL} terms. (More generally, this approximation applies as long as $k_{h,g} \gg -a$.) This leads immediately to the solution (3) in the main text.

POLYMER REORGANIZATION TIME

Here we estimate the reorganization time for polymers to disassemble at one spatial site (site 1) and reassemble at another spatial site (site 2) following a switch in nucleation. As defined in the main text, the reorganization time is the time needed after the switch for half of the final steady-state amount of polymerized material to assemble at site 2. For fast monomer diffusion, we estimated the reorganization time in the main text as half the average material age.

When diffusion is slow, we must estimate the reorganization time differently. For equilibrium polymers, after the switch in nucleation, site 1 comes to a local quasi-steady-state free monomer concentration: as diffusion slowly drains the free monomer pool at site 1, depolymerization keeps the free monomer concentration roughly constant. The quasi-steady-state free monomer concentration c_1 is

$$c_1 = \frac{k_-}{k_+}. \quad (\text{S10})$$

At site 2, the free monomer concentration also quickly comes to a value that stays roughly constant for a long time. However, this value is smaller than c_1 since nucleation removes free monomers from the pool at site 2. We may estimate this free monomer concentration c_2 roughly by

$$k_- N_2 - k_+ c_2 N_2 - 2k_{\text{nucl}} c_2^2 = 0, \quad (\text{S11})$$

$$k_{\text{nucl}} c_2^2 - \frac{N_2}{\text{MFPT}} = 0, \quad (\text{S12})$$

where N_2 is the number of polymers at site 2. Although N_2 , like c_2 , is time-dependent and slowly grows as diffusion moves monomers from site 1 to site 2, immediately after the switch N_2 quickly comes to a value that stays roughly constant for a long time. Using this value, which is approximately half the final expected steady-state number of polymers, and using the final expected MFPT (which is the same as before the switch in nucleation), we may come up with a rough estimate for c_2 . Then an estimate for the reorganization time is just the time needed for half the final steady-state amount of polymerized material to diffuse down the concentration ‘‘gradient’’ from site 1 to site 2. If c_{steady} is the final steady-state concentration of polymerized material, then our estimate for the reorganization time may be written as

$$\tau_{\text{reorg}}^{\text{equil}} \approx \frac{c_{\text{steady}}/2}{k_D(c_1 - c_2)}. \quad (\text{S13})$$

For typical parameter values (such as those used in Fig. 2D), we find that this estimate for the equilibrium-polymer reorganization time is accurate to within a factor of 2.

For active polymers, after the switch in nucleation, site 1 can replenish the free monomer pool only by polymer disassembly. Since diffusion is slow, monomers released by disassembly typically rejoin other polymers at site 1. Hence after the switch, the number of active polymers at site 1 rapidly drops while the average polymer length grows, until eventually site 1 has only a few very long, very long-lived polymers. These few long-lived polymers then quickly accumulate and hydrolyze all the free monomers at site 1, and then all the polymers disassemble. Therefore, a rough estimate for the reorganization time is just the time needed to hydrolyze all the monomers at site 1, plus the time needed for half of that material to diffuse to site 2:

$$\tau_{\text{reorg}}^{\text{active}} \approx \frac{c_{\text{total},1}}{k_h} + \frac{1}{2k_D}, \quad (\text{S14})$$

where $c_{\text{total},1}$ is the initial total concentration of material at site 1. For typical parameter values (such as those used in Fig. 2D), this estimate for the active-polymer reorganization time is accurate to better than 10%.

COMPARISON OF EQUILIBRIUM AND ACTIVE-POLYMER LENGTH DISTRIBUTIONS WITH THE SAME AVERAGE LENGTH

In Fig. 2B, we showed that equilibrium and active polymers with the same MFPT have qualitatively different length distributions: the active polymers have a much longer average length. Figure S2 shows that even for equilibrium and active polymers with the same average length, there are more very long active polymers than very long equilibrium polymers.

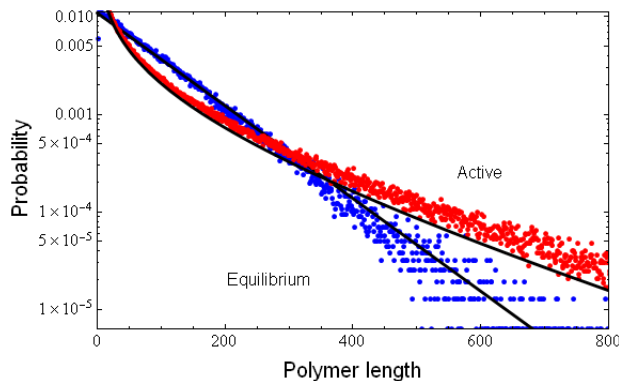


Figure S2: Histogram of lengths for equilibrium (blue) and active (red) polymers with average length $\simeq 90$. Black curves are theoretical fits from (5) and (7).

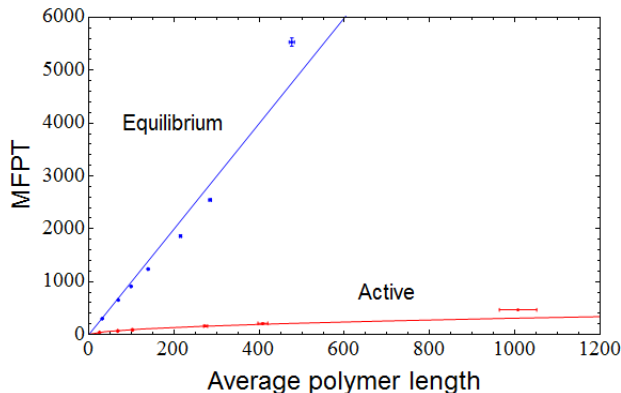


Figure S3: MFPT versus average length for equilibrium (blue) and active (red) polymers, with the steady-state fraction of polymerized material held at 95%. Curves are theoretical fits using $\text{MFPT} = \frac{2}{D} \langle L \rangle_{\text{equil}}$ for equilibrium polymers and (6) for active polymers.

MFPT VERSUS AVERAGE LENGTH FOR 95% POLYMERIZED MATERIAL

In the simulations described in the main text, we adjusted the nucleation rate k_{nucl} so that the steady-state fraction of polymerized material was always held fixed at 75%. For comparison, Fig. S3 shows the MFPT of equilibrium and active polymers as functions of their average length, akin to Fig. 2A, with the steady-state fraction of polymerized material held instead at 95%. The general trends are the same as those seen in Fig. 2A: for a given average length, active polymers disassemble significantly faster than equilibrium polymers in a manner well-predicted by Fokker-Planck theory, and the difference increases as average length increases. The MFPT is measured in the same time units as defined in the main text, even though the steady-state free monomer concentration is different.

MFPT VERSUS AVERAGE LENGTH FOR PARTIALLY-VECTORIAL HYDROLYSIS AND FINITE DEPOLYMERIZATION VELOCITY

In the simulations described in the main text, we studied a minimal microtubule model with vectorial hydrolysis (i.e. only the last monomer in the polymer cap is subject to hydrolysis) and infinite depolymerization velocity when the polymer cap size goes to zero. Here we relax these assumptions. First, we consider the more realistic partially-vectorial microtubule model described by Flyvbjerg, Holy, and Leibler (FHL) [1]. This model has a vectorial hydrolysis rate k_h for any GTP-bound monomer adjacent to a GDP-bound monomer (i.e. identical to our minimal model), and a smaller non-vectorial hydrolysis rate $r = k_r/\delta x$ for all other GTP-bound monomers, representing the rate per unit length at which new GTP-GDP interfaces are created. $\delta x \simeq 8\text{nm}$ is the length scale of an individual tubulin monomer. In all other respects the FHL model is identical to our own.

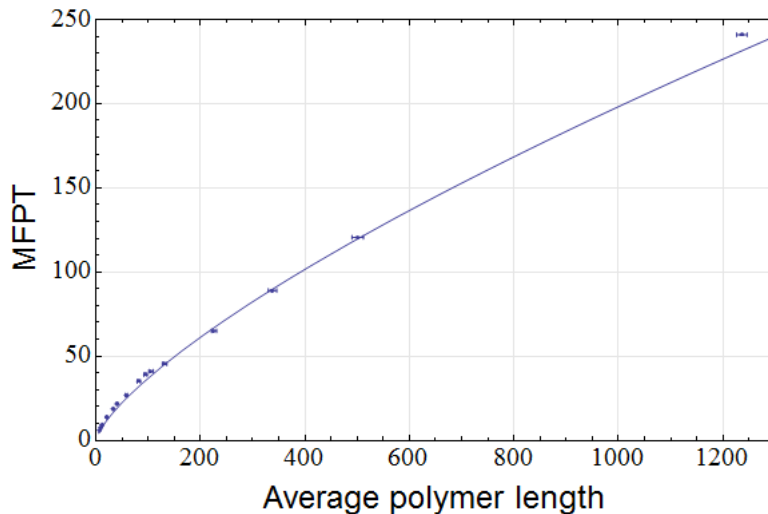


Figure S4: MFPT versus average length for the FHL model [1]. Curve is a numerical fit to a power law, $\text{MFPT} \sim \langle L \rangle^{0.7}$.

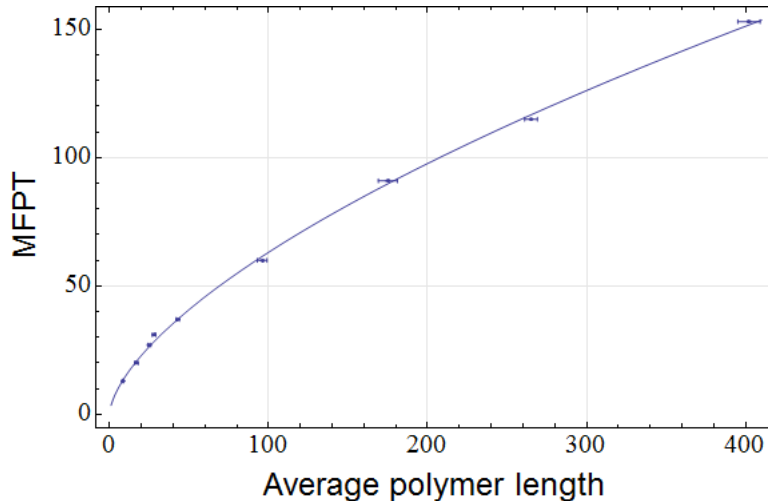


Figure S5: MFPT versus average length for the modified FHL model [1] with finite zero-cap depolymerization rate. Curve is a numerical fit to a power law, $\text{MFPT} \sim \langle L \rangle^{0.7}$.

Figure S4 shows the MFPT versus average length for polymers in this more realistic microtubule model, akin to Fig. 2A. In these simulations $k_r = k_h/10$, roughly the value FHL found by fitting to experimental data. The MFPT scales $\sim \langle L \rangle^{0.7}$, in between the $\sim \langle L \rangle^{1/2}$ scaling of our purely vectorial model and the $\sim \langle L \rangle$ equilibrium scaling.

Since the FHL paper did not consider microtubule disassembly dynamics (the purpose of the paper was only to predict the distribution of polymer catastrophe times), we next consider the effect of adding to this model a finite depolymerization rate $k_-^{(\text{dep})}$ representing the rate of polymer disassembly after the cap size goes to zero. We choose $k_-^{(\text{dep})}$ to be twice the polymerization rate k_{+c} . All other parameters are the same as in the other FHL simulations above. Figure S5 shows the MFPT versus average length in this modified FHL model. Again the MFPT scales $\sim \langle L \rangle^{0.7}$.

Hence, the MFPT scales sublinearly with mean polymer length in a more realistic non-equilibrium microtubule model. We did find two regimes that produce linear scaling in the modified FHL model: if the average depolymerization time for the entire polymer is much longer than the average time for the cap size to reach zero, then the MFPT is dominated by the depolymerization time and scales linearly with average length (data not shown). However, this is not the regime observed experimentally for microtubules [2]. Also, if the vectorial hydrolysis rate goes to zero (i.e. the hydrolysis rate is the same for all GTP-bound monomers), then the MFPT scales linearly with the average length (data not shown), but this is not thought to be the case for microtubules.

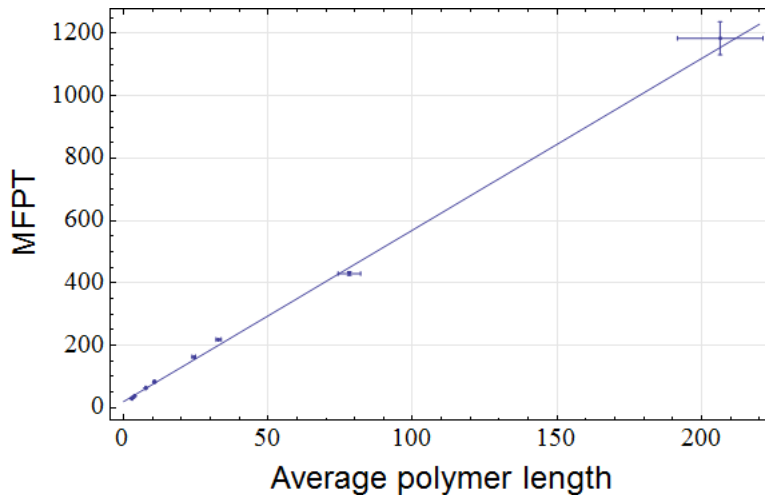


Figure S6: MFPT versus average length for the two-species equilibrium model in the regime where one monomer type is energetically favored over another. This regime is designed to mimic our non-equilibrium model from the main text. Curve is a numerical fit to a linear relationship, $\text{MFPT} \sim \langle L \rangle$.

MFPT VERSUS AVERAGE LENGTH FOR TWO-SPECIES EQUILIBRIUM POLYMER

In the main text we argued that a large class of equilibrium polymer models produces mean lifetimes that scale linearly with mean lengths. This class includes all equilibrium polymers comprised of an ordered sequence of monomers, each of one of q types or conformations (or q^k types for k protofilaments), where interactions between neighboring monomers $\{i, i + 1\}$ contribute free energy $J_{\{i, i+1\}}$ to the total free energy of the polymer. This class maps one-to-one onto 1-d, q^k -state Potts models, and produces a free energy that scales linearly with mean length.

To provide further validation for our argument, we simulated one such equilibrium model with $q = 2$ different monomer types. This model is designed to be the equivalent of our minimal non-equilibrium microtubule model, but subject to the equilibrium constraint of reversibility. Specifically, monomers of one type (the “GTP-bound” type) can attach and detach at the front of the polymer. Monomers at the back of the cap can interconvert between the two types, and when the cap size goes to zero (i.e. when the polymer is entirely composed of monomers of the “GDP-bound” type), monomers of the “GDP-bound” type can both attach and detach.

First we consider an energetic regime comparable to our non-equilibrium model. We set the energy of “GTP-bound” monomers to favor attachment, and that of “GDP-bound” monomers to favor detachment. This means that “GTP-bound” monomers are more stable in polymers, and “GDP-bound” monomers are more stable as free monomers. However, in order for monomer interconversion to occur mainly from “GTP-bound” to “GDP-bound”, as for the non-equilibrium system, “GDP-bound” monomers must also be more stable than “GTP-bound” monomers even in polymers. This implies that the total monomer population will consist mostly of “GDP-bound” monomers. Indeed, when simulated in this regime, with the same overall k_+ and fraction of polymerized material as in our original simulations, we find a ratio of “GDP-bound” monomers to “GTP-bound” monomers of 10:1. Furthermore, in the limit where monomer interconversion approaches unidirectional from “GTP-bound” to “GDP-bound”, the system approaches a single species, and we recover our original equilibrium model. Finally, Fig. S6 shows the MFPT versus average length for this two-species equilibrium model. The MFPT scales linearly with average length as expected.

Second we consider the regime where the two monomer species are energetically equivalent. Figure S7 shows the MFPT versus average length for this model. Again the MFPT scales linearly with average length as expected.

* Electronic address: dsswanso@princeton.edu

† Electronic address: wingreen@princeton.edu

[1] H. Flyvbjerg, T. E. Holy, and S. Leibler, *Phys. Rev. Lett.* **73**, 17 (1994).

[2] R. A. Walker, E. T. O’Brien, N. K. Pryer, M. F. Soboeiro, W. A. Voter, H. P. Erickson, and E. D. Salmon, *J. Cell Biol.* **107**, 4 (1988).

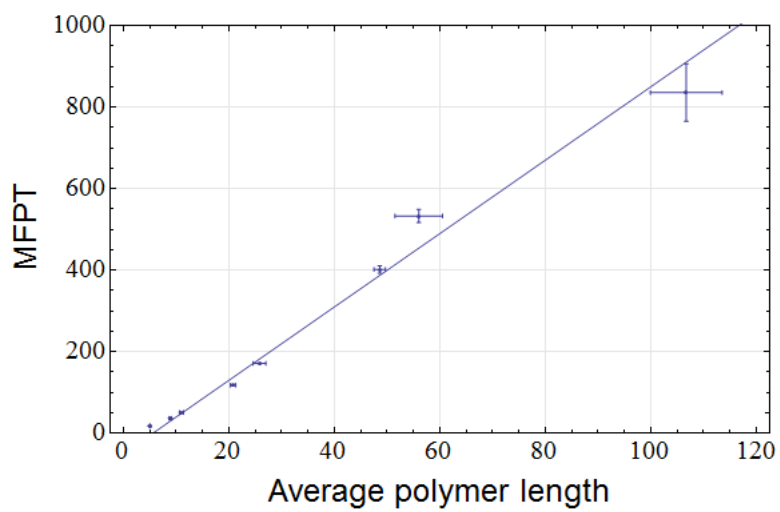


Figure S7: MFPT versus average length for the two-species equilibrium model in the regime where the monomer types are energetically equivalent. Curve is a numerical fit to a linear relationship, $\text{MFPT} \sim \langle L \rangle$.